



THE UNIVERSITY *of* EDINBURGH

Edinburgh Research Explorer

Machine learning approach for analysing and predicting the modulus response of the structural epoxy adhesive at elevated temperatures

Citation for published version:

Wang, S, Xu, Z, Stratford, T, Li, B, Zeng, Q & Su, J 2023, 'Machine learning approach for analysing and predicting the modulus response of the structural epoxy adhesive at elevated temperatures', *The Journal of Adhesion*. <https://doi.org/10.1080/00218464.2023.2183851>

Digital Object Identifier (DOI):

[10.1080/00218464.2023.2183851](https://doi.org/10.1080/00218464.2023.2183851)

Link:

[Link to publication record in Edinburgh Research Explorer](#)

Document Version:

Peer reviewed version

Published In:

The Journal of Adhesion

General rights

Copyright for the publications made accessible via the Edinburgh Research Explorer is retained by the author(s) and / or other copyright owners and it is a condition of accessing these publications that users recognise and abide by the legal requirements associated with these rights.

Take down policy

The University of Edinburgh has made every reasonable effort to ensure that Edinburgh Research Explorer content complies with UK legislation. If you believe that the public display of this file breaches copyright please contact openaccess@ed.ac.uk providing details, and we will remove access to the work immediately and investigate your claim.



1

2 **Machine learning approach for analysing and predicting the modulus**

3 **response of the structural epoxy adhesive at elevated temperatures**

4 S. Wang^{a,b,*}, Z. Xu^{a,b}, T. Stratford^c, B. Li^{a,b}, Q. Zeng^{a,b}, J. Su^{a,b}

5 ^a School of Civil Engineering, Architecture and Environment, Hubei University of Technology, Wuhan 430068, China

6 ^b Innovation Demonstration Base of Ecological Environment Geotechnical and Ecological Restoration of Rivers and Lakes,
7 Hubei University of Technology, Wuhan 430068, China

8 ^c School of Engineering, Institute for Infrastructure and Environment, The University of Edinburgh, Edinburgh EH9 3FG,
9 UK

10
11 Email: wangsongbo@hbut.edu.cn (S. Wang)

13 **Abstract**

14 For bonded Fibre Reinforced Polymer (FRP) strengthening systems in civil engineering
15 projects, the adhesive joint performance is a key factor in the effectiveness of the strengthening;
16 however, it is known that the material properties of structural epoxy adhesives change with
17 temperature. This present paper examines the implied relationship between the curing regimes
18 and the storage modulus response of the adhesive using a Machine Learning (ML) approach.
19 A dataset containing 157 experimental data collected from the scientific papers and academic
20 theses was used for training and testing an Artificial Neural Network (ANN) model. The
21 sensitivity analysis reveals that the curing conditions have a significant effect on the glass
22 transition temperatures (T_g) of the adhesive, and consequently on the storage modulus response
23 at elevated temperatures. Curing at an extremely high temperature for a long time does not,
24 however, guarantee a better thermal performance. For the studied adhesive, curing in a warm
25 ($\geq 45^\circ\text{C}$) and dry (near 0 % RH) environment for 21 days is recommended for practical
26 applications. A software with a Graphical User Interface (GUI) was established, which can
27 predict the storage modulus response of the adhesive, plot the corresponding response curve,
28 and estimate the optimum curing condition.

29

30 **Keywords:** Structural epoxy adhesive; Curing conditions; Storage modulus; Machine learning;
31 Artificial neural network.

32

33 **1 Introduction**

34 The civil engineering industry has witnessed a rapid growth in the use of externally bonded
35 composite materials to strengthen structures across the world [1–3]. This has stimulated the use
36 of structural epoxy adhesives in civil structures, as it can offer the advantages of low additional
37 weight, more uniform stress distribution, and design flexibility, when compared to
38 conventional joining techniques [4–6]. However, when the ambient temperature increases,
39 adhesive joints may perform differently than at a normal temperature, as the glass transition
40 behaviour of the adhesive layer will result in a reduction in its strength and stiffness,
41 consequently reducing the stress transfer capacity of the joint [7–10].

42 Traditional experimental investigations on the performance of adhesive layers can
43 sometimes inevitably lack representativeness and generalisation. Using Machine Learning (ML)
44 approaches enables the incorporation of available experimental results into an unified model,
45 without the need for individual testing at each data point, which provides a more
46 comprehensive and systematic understanding on the existing results. Through extracting
47 complicated relationships between parameters and outputs, ML can further summarise implicit
48 nonlinear laws and apply them to make new predictions, without involving labour-intensive
49 work [11–13].

50 The first concept of ML was introduced in 1959 by Arthur Samuel [14], who defined ML
51 as a field of study that enables computers to have the ability to learn without being explicitly
52 programmed [15]. Since the 1990s, engineers have been using ML techniques to explore the
53 complex behaviour of structural materials, among which artificial neural network (described

54 further in Section 2) in one of the most widely used ML methods. For example, Ghaboussi et
55 al. [16] successfully used an Artificial Neural Network (ANN) in 1991 to predict the behaviour
56 of concrete subjected to certain loading paths, while Rao and Mukherjee [17] used an ANN in
57 1996 to predict the micromechanical response of ceramic matrix composites [12,18].

58 Over the last decade, several studies have been carried out using ML ANN approaches to
59 analyse the response of adhesively bonded joints, particularly for single lap-shear joints. A
60 back-propagation ANN model for predicting the bond strength of Fibre Reinforced Polymer
61 (FRP)-to-concrete joints was first proposed by Mashrei et al. [19] in 2013. Tosun and Çalık
62 [20] developed an ANN model to estimate the strength of aluminum-to-aluminum single lap-
63 shear joints based on their geometric dimensions in 2016, while in 2021, Gu et al. [5] further
64 developed an upgraded ANN predictive model, which comprehensively considers the
65 combined effects of continuous and discrete design (geometry and material) variables. Besides
66 these, ANN approach can also be applied to develop constitutive material models for adhesive
67 bonds. For instance, the rate dependent response of bonded joints was studied by Zgoul [21]
68 using a proposed ANN constitutive model; and most recently, a ML material model that can
69 be used in finite element analysis to estimate the element failure was developed by Sommer et
70 al. [18]. These studies demonstrate the reliability of the ML ANN approach; however, they
71 have been constrained to adhesively bonded joints rather than the structural adhesive itself and
72 neither of them considers the effects of curing conditions or elevated environmental
73 temperatures.

74 Studies using ML approaches to explore the thermal performance of structural epoxy
75 adhesives are rare. Jha et al. [22] and Tao et al. [23] were dedicated to establishing correlations
76 between the chemical structure and the glass transition behaviour of polymers. Szabelski et al.
77 [24] applied the ANN method to investigate the influences of adhesive mixing ratios and curing
78 conditions on the tensile strength of bonded joints. The results indicated that the higher curing

79 temperature resulted in a relatively higher tensile strength, but the higher test temperature
80 resulted in a significantly lower tensile strength. This demonstrates the importance of studying
81 the mechanical behaviour of adhesives in relation to their curing conditions and service ambient
82 temperatures. So far, there is a lack of research using machine learning approaches to analyse
83 the implicit relationship between the modulus response of adhesives and the applied curing
84 conditions.

85 The aims of this study are to explore the influence of elevated temperatures on the storage
86 modulus response of the structural epoxy adhesive, and how the applied curing conditions
87 related to the thermal performance of the adhesive. This is achieved by utilising the ML
88 approach, as the traditional curve fitting method is not applicable due to the complexity of the
89 T_g behaviour, the curing regimes, and the variety of different test data. The ML approach can
90 enable a better understanding of experimental data and incorporate them into a unified model
91 for further comprehensive analysis and prediction of the thermal response of the adhesive. The
92 predictions obtained without conducting time-consuming and expensive experimental tests can
93 provide reference values for practical engineering applications.

94 A predictive ANN model is proposed to map the relationship between the modulus response
95 and the curing conditions. And for the first time, a user-friendly software with a Graphical User
96 Interface (GUI) which implements the proposed ANN model is developed.

97

98 **2 Artificial Neural Network (ANN)**

99 ANN is a machine learning technique with flexible mathematical structures inspired by the
100 networks of biological neurons in human brains. A typical ANN system comprises one input
101 layer, one or more hidden layers and one output layer. After training, the system is capable of
102 identifying complex nonlinear relationships between input and output data [9,25,26].

103 As shown in Figure 1, like biological neurons receiving signals from dendrites, all input
 104 parameters obtained from the dataset form the input layer of the ANN. The received parameters
 105 information is gathered in the hidden layer(s) and modulated through an activation function
 106 before being output to the output layer. This process can be expressed as follows [9,26,27]:

$$107 \quad y_i = \sigma \left(\sum_{i=1}^n W_i^k I_i + b_i \right) \quad (1)$$

108 where y_i refers to the output of neuron i , I_i refers to its input, σ is the activation function,
 109 W_i^k represents the weight, and b_i represents the bias [26].

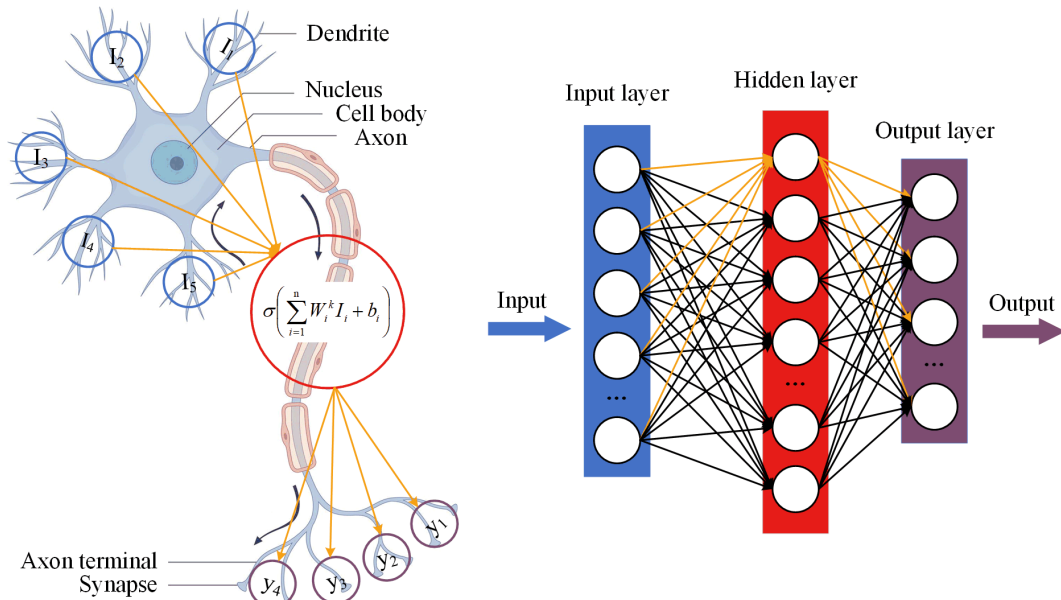


Figure 1: The schematic illustration of an ANN structure

112 The number of neurons varies greatly among different problem cases, and therefore, trial
 113 and error is necessary to determine the structure of the ANN network before the network
 114 training. The goal of training an ANN is to minimise the network error by optimising the weight
 115 factors (W_i^k) that represent the strength of connections between neurons. Mean Square Error
 116 (MSE) is one of the criteria used to evaluate the performance of a network [9,26,28]:

$$117 \quad MSE = \frac{1}{N} \sum_{i=1}^N (t_i - \bar{y}_i)^2 \quad (2)$$

118 where N is the number of data, t_i is the target value, \bar{y}_i is the predicted value. The training
119 process is iterative, where \bar{y}_i is estimated by assigning a random weight (W_i^k) value each time,
120 and the corresponding MSE is calculated. The initial weight (W_i^k) value is continuously
121 updated until the MSE falls within a satisfactory range, and this is known as a back-propagation
122 algorithm [26,28,29].

123 The basic concepts of the ANN machine learning technique have been clarified above, and
124 more detailed information can be found in the cited references. In the next section, the
125 development of the datasets is presented.

126

127 **3 Data acquisition and pre-processing**

128 Dynamic Mechanical Analysis (DMA) is a widely used technique for measuring the storage
129 modulus of materials as a function of temperature [30,31], which has been used in a number of
130 studies to determine the thermal properties of adhesives. In the present paper, the DMA
131 experimental results of a structural epoxy adhesive (Sikadur-330 [32]) were extracted from a
132 total of 11 scientific papers and academic theses to form two datasets. Dataset A containing
133 157 experimental results was used to develop the ANN model, while dataset B containing 6
134 experimental results was used to carry out subsequent validation work.

135 The adhesive, Sikadur-330, selected for this study is an ambient-cured epoxy that is
136 frequently used to apply FRP-bonded strengthening in infrastructure projects. The material
137 consists of a thixotropic, solvent-free, bi-component epoxy-based adhesive, and its chemical
138 structure comprises a bisphenol-A based epoxy resin and aliphatic amines as hardeners, with
139 small amounts of silica-based fillers. The recommended mixing ratio in weight of the resin to
140 the hardener is 4:1 in the material data sheet [32,33].

141 Establishing a ML model for all types of structural adhesives was not possible within the
142 scope of the current project, which would require a separate research work to collect an
143 extremely massive database. Nevertheless, the research methodology demonstrated in this
144 paper and the obtained implied relationship between parameters and outputs can provide a
145 useful reference for studying other structural adhesives.

146

147 **3.1 Critical points for analysing the modulus response**

148 An indirect data training approach was used in this study, as the modulus response is a
149 continuous result that cannot be used directly to generate the output part of the dataset. A
150 summative output part with limited variables is required to prevent overfitting issues [34].
151 Figure 2 illustrates an example of the temperature-dependent storage modulus curve (black line)
152 of the adhesive obtained from a DMA test [35], where the five critical modulus points related
153 to the glass transition temperature (T_g) of the adhesive are marked:

- 154 • Initial modulus (E1): the storage modulus at room temperature (around 20 °C);
- 155 • Modulus corresponding to Onset T_g (E2): the intersection of two lines tangent to the
156 glassy and leathery portions of the modulus response curve [30,36];
- 157 • Modulus corresponding to Inflection point T_g (E3): the point of inflection of the
158 leathery portion of the curve [30,36];
- 159 • Modulus corresponding to Peak $\tan \delta T_g$ (E4): the modulus at which the maximum
160 $\tan \delta$ (the ratio of loss modulus to storage modulus) occurs [30,36];
- 161 • Final modulus (E5): the storage modulus stabilises at the highest temperature
162 (approximately 100 °C).

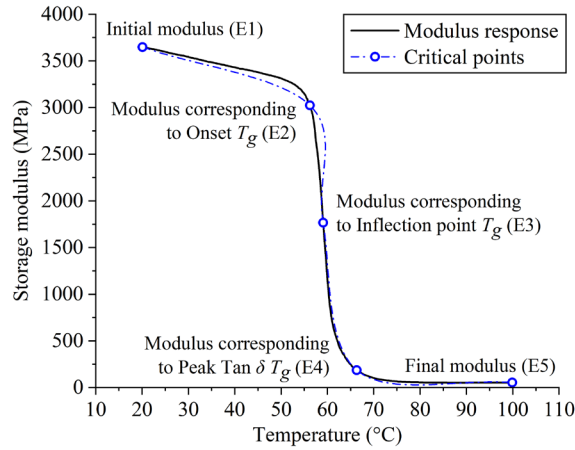


Figure 2: Simplify the modulus variation at elevated temperatures using the critical points

163
164

165 The entire temperature-dependent modulus response curve can be estimated by connecting
 166 the five critical points. As shown by the blue line in the figure, the estimated curve was
 167 generated using the modified Bezier line connection method in the Origin Lab software [37].
 168 The corresponding five critical points data were therefore extracted from the experimental
 169 results in the literature to form the summative output parts of the datasets. Note that the
 170 obtained five critical points data were not filtered, which ensured the authenticity of the created
 171 dataset, although there may have been slight errors during the process of extracting the data
 172 (E1-E5) by drawing the auxiliary lines manually.

173

174 3.2 The development of the datasets

175 Table 1 summarizes the literature used to construct the dataset A and dataset B. 157 DMA
 176 experimental results from 9 references (dataset A) were used to develop (through training and
 177 testing) the ANN model (described in Section 4), and the other 6 results from 2 references
 178 (dataset B) were used to validate the established user-friendly software (described in Section
 179 6). The DMA tests were carried out by applying dynamic flexural loads to the samples. A more
 180 detailed description of each test can be found in the cited references listed in Table 1. The
 181 experimental data from Othman's research at the University of Edinburgh [38] forms a large
 182 part of the datasets, which is due to the lack of other comprehensive experimental studies on

183 the effect of different curing conditions on the modulus response of the studied adhesive.
 184 Whilst a more comprehensive dataset would be preferable, additional experimental work was
 185 beyond the scope of this study.

186 Table 1: Reviewed literature for constructing the datasets

No.	Reviewed Literature	No. of samples
1	Othman [38]	144
2	Wang et al. [10]	3
3	Wang et al. [35]	1
4	Sousa et al. [33]	1
5	Seif et al. [39]	1
6	Sun et al. [40]	3
7	Verdet et al. [41]	1
8	Lartigau et al. [42]	1
9	Savvilotidou et al. [43]	2
(Dataset A: 157 samples for developing the ANN model)		
10	Stratford and Bisby [7]	5
11	Burke et al. [44]	1
(Dataset B: 6 samples for validating the established software)		

187
 188 The raw data of the dataset A and dataset B are listed in the supplementary material. Table
 189 2 presents the features of the dataset A used for developing the ANN model.

190 Table 2: Statistical summary of the dataset A used for developing the ANN model

Variables	Min	Mean	Max	Coefficient of variation
<i>Inputs</i>				
Curing temperature (°C)	13	43.6	80	52.1%
Curing time (days)	3	13.2	34	73.5%
Curing humidity (%)	0	49.5	100	97.0%
<i>Outputs</i>				
E1: Initial modulus (MPa)	1952.9	3136.4	4172.9	14.2%
Onset T_g (°C)	28.5	52.3	74.9	22.6%
E2: Modulus corresponding to Onset T_g (MPa)	1111.6	2273.0	3281.7	21.3%
Inflection point T_g (°C)	34.9	58.8	80.3	21.1%
E3: Modulus corresponding to Inflection point T_g (MPa)	649.9	1289.4	2107.3	22.9%
Peak $\tan \delta T_g$ (°C)	46.5	67.3	89.1	17.5%
E4: Modulus corresponding to Peak $\tan \delta T_g$ (MPa)	66.5	234.6	575.6	46.2%
E5: Final modulus (MPa)	19.9	40.2	78.2	34.8%

191
 192 The raw data needs to be normalised at the pre-processing stage, which can accelerate ANN
 193 training and improve prediction accuracy, especially for this study where the ranges of values
 194 of the variables (inputs and outputs) are significantly different. The min-max scaling method
 195 is applied [5,9]:

$$X' = \frac{X - X_{min}}{X_{max} - X_{min}} \quad (3)$$

197 where X represents the raw data, X' represents the normalised data, X_{min} and X_{max} refer to
198 the minimum and maximum values of the target variable in the whole dataset. The full
199 normalised dataset A is listed in the supplementary material as well.

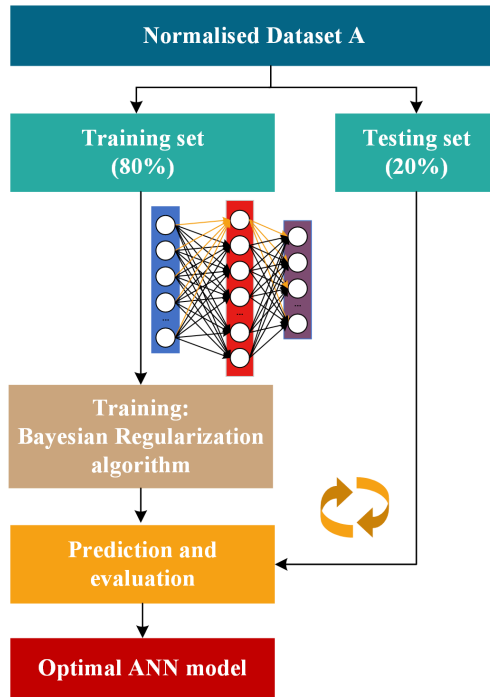
200

201 **4 Establishment of the ANN model**

202 The construction process of the ANN model is shown in Figure 3. The Bayesian
203 Regularization algorithm was used to train the ANN, which randomly divided the applied
204 dataset A into two parts, 80% (126 samples) for training and 20% (31 samples) for testing.
205 Whilst this algorithm usually requires more time, it can minimise the combination of squared
206 errors and weights to train an ANN that performs reasonable generalisation for difficult, small,
207 or noisy datasets [45,46]. The proposed ANN consists of one input layer, one hidden layer and
208 one output layer. The activation functions for the hidden and output layers adopted the
209 TANSIG (Equation (4)) function and the PURELIN function (Equation (5)), respectively. The
210 TANSIG function produces data values between [-1, +1], while the PURELIN function keeps
211 the inputs constant [28,45].

$$212 \quad y = \text{TANSIG}(x) = \frac{2}{(1 + e^{-2x})} - 1 \quad (4)$$

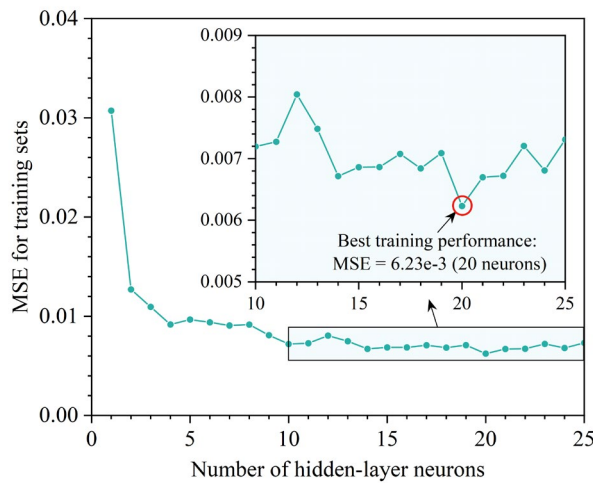
$$213 \quad y = \text{PURELIN}(x) = x \quad (5)$$



214
215

Figure 3: Construction process of the ANN model

216 The number of hidden-layer neurons was determined through trial and error. As shown in
 217 Figure 4, 20 neurons were applied to construct the ANN model as this resulted in the lowest
 218 MSE (Equation (2)).



219
220

Figure 4: Training mean squared error with different numbers of hidden-layer neurons

221

222 5 Results and discussions

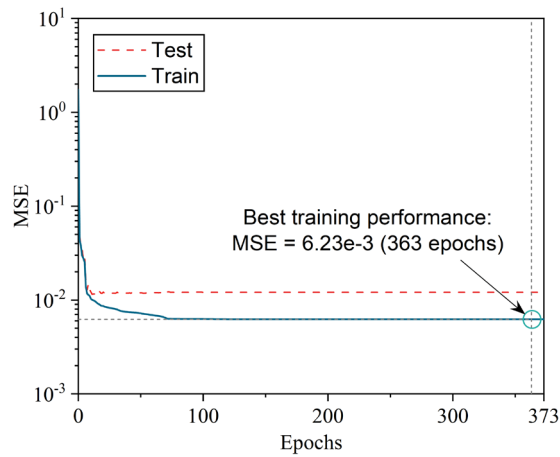
223 In this section, the performance of the ANN model is presented, and the predicted results of
 224 the modulus response are compared with the experimental results from the literature to verify

225 the model. The complex relationship between the curing conditions and the modulus response
226 is then analysed using the developed ANN model.

227

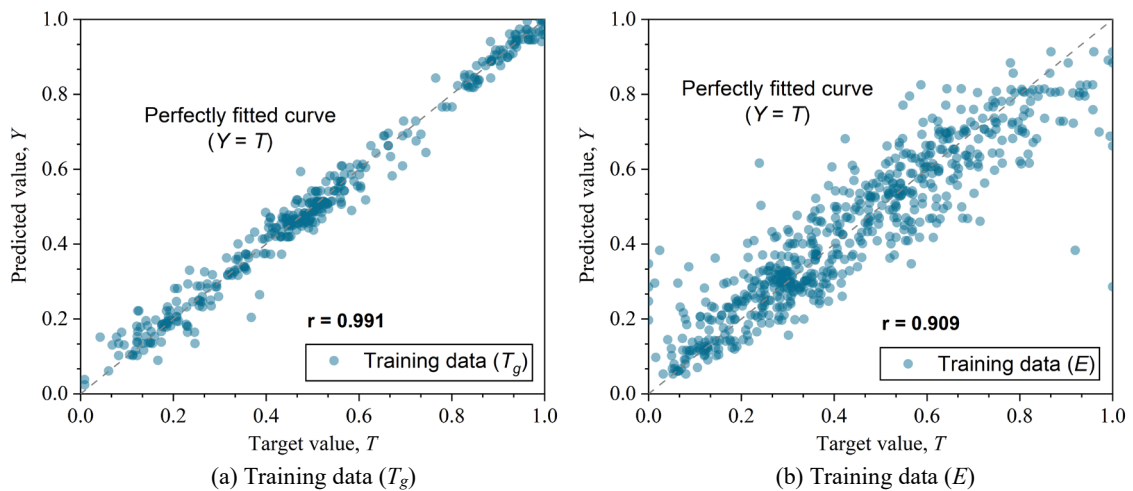
228 5.1 Model performance evaluation

229 Figure 5 illustrates the best training performance of the ANN model, which was obtained at
230 the 363rd epochs with the MSE (Equation (2)) equals to 6.23e-3. The corresponding regression
231 diagrams of the training set and testing set at the 363rd epochs are shown in Figure 6, where Y
232 and T refer to the normalised predicted values and target values.



233
234

Figure 5: ANN training performance



235
236

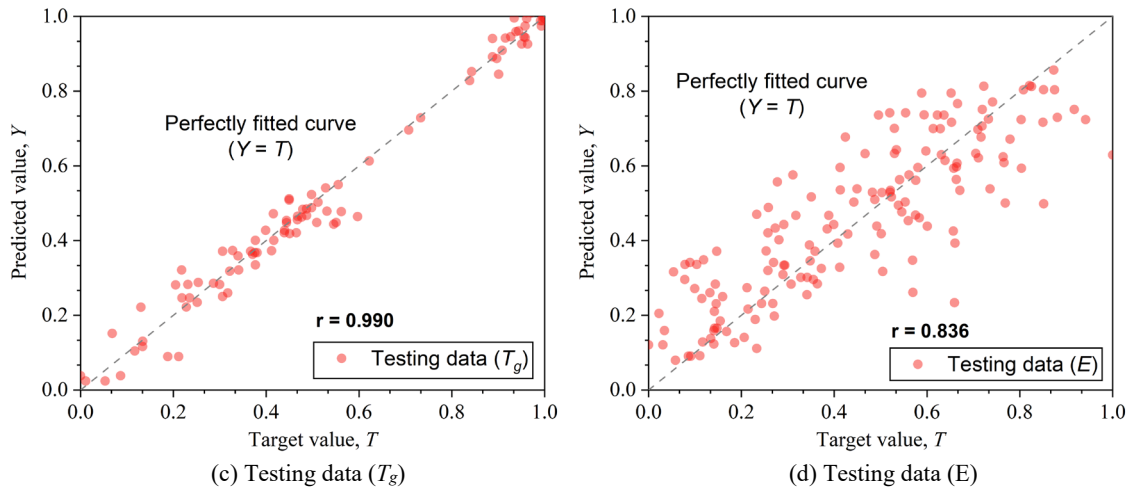


Figure 6: Regression of the developed ANN model

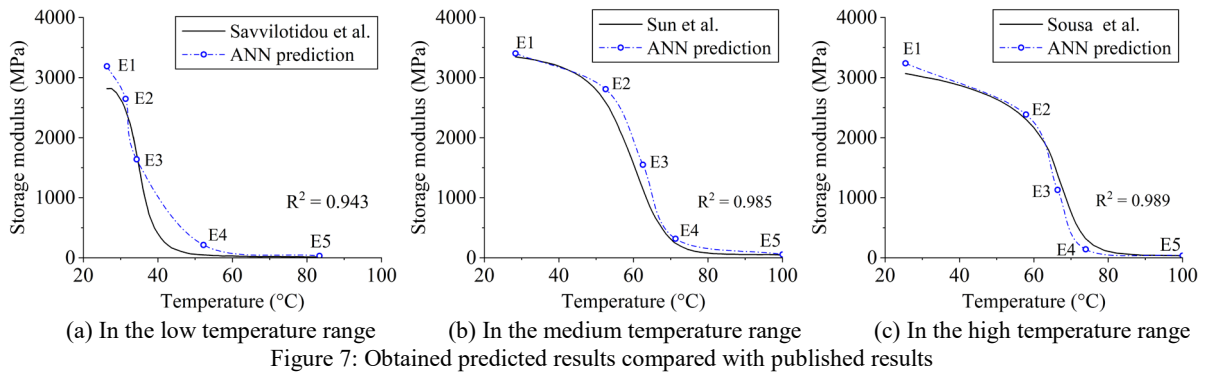
237
238
239

240 The correlation coefficients (r) corresponding to the T_g values (Onset T_g , Inflection point T_g ,
241 and Peak $\tan \delta T_g$) were higher than those corresponding to the modulus values (E1 – E5),
242 which indicates that the trained ANN model was able to predict the adhesive's T_g values more
243 accurately. Nevertheless, the overall response with the correlation coefficients close to 1.0
244 suggested that the training produced the optimal results.

245

246 5.2 Verification of the developed ANN model

247 The predicted values need to be post-processed to obtain the modulus response of the
248 adhesive due to the indirect data training approach used in developing the ANN model. The
249 comparison of the predicted modulus response curves (using the modified Bezier line
250 connection method in the Origin Lab software [37]) and the experimental results (storage
251 modulus versus temperature curves) from scientific papers are shown in Figure 7. The three
252 selected representative comparison results correspond to the glass transition behaviour
253 occurring in the low, medium, and high temperature ranges. The coefficient of determination
254 (R^2) of each comparison is illustrated in Figure 7.



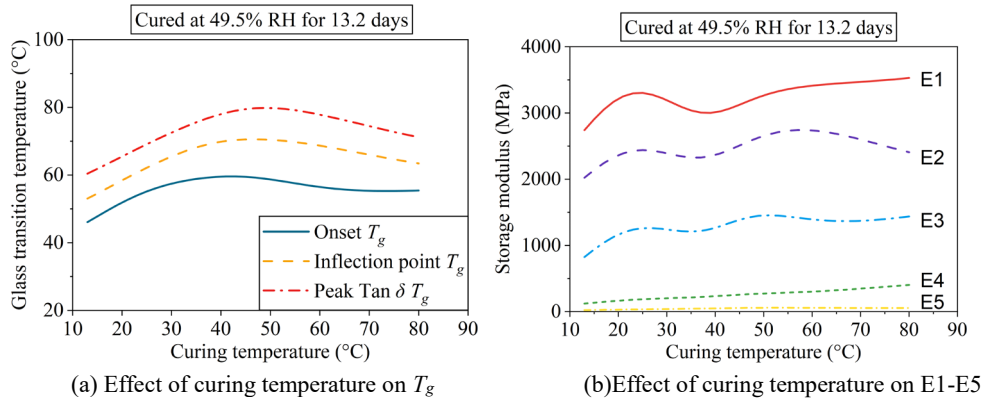
258 The predicted modulus response of the adhesive at elevated temperatures is suitably accurate
259 from the viewpoint of engineering practice. The ANN model developed using the dataset A
260 (Table 1), which contains a large proportion of data from Othman's experiments [38], can also
261 be used to accurately predict the results from other experiments, demonstrating the great
262 generality of the ANN machine learning approach. Note, however, that for the glass transition
263 behaviour occurring in the low temperature range, if the precise modulus response is of
264 interests, an extra experiment may still be necessary.

265

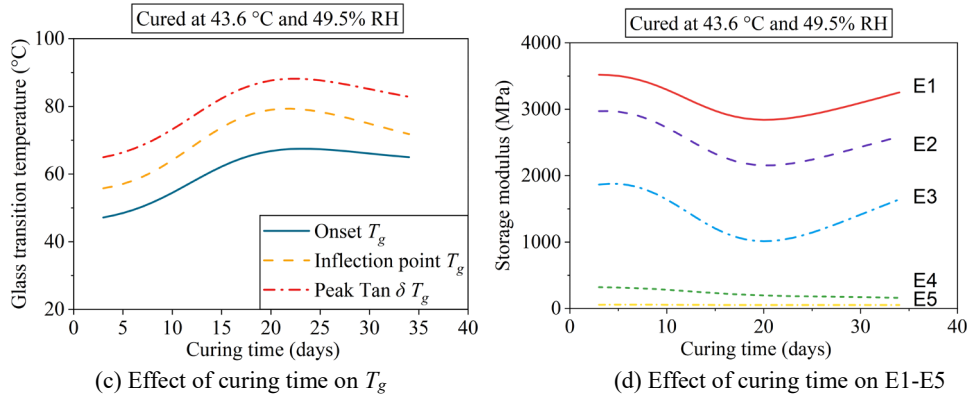
266 5.3 The effect of curing conditions on the modulus response at elevated temperatures

267 The developed ANN model made it possible to obtain a substantial number of predictions
268 conveniently, which allowed for a comprehensive analysis of the relationship between the
269 curing conditions (inputs) and the modulus response at high temperatures (outputs). The effects
270 of curing temperature, curing time, and curing humidity, respectively, on the T_g and modulus
271 values of the adhesive are visualised in Figure 8. The benchmark curing condition was set at
272 43.6 °C and 49.5% RH for 13.2 days, based on the mean values of the variables in the dataset
273 A (see Table 2).

274
275



276
277



278
279
280

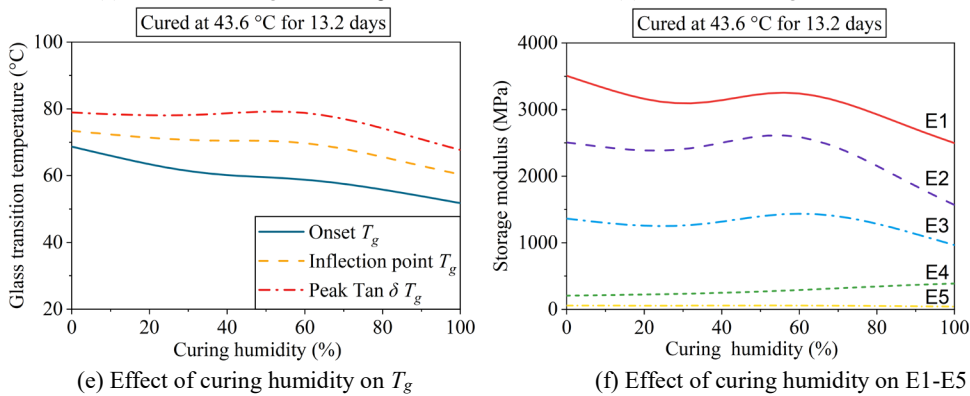


Figure 8: The effect of curing conditions on the critical points of modulus response at elevated temperatures

281
282
283
284
285
286
287
288

- As shown in Figure 8 (a), by keeping the benchmark curing time and curing humidity constant, as the curing temperature increases from 13 °C, the crosslinking of the epoxy adhesive increases and the free volume decreases, which results in the T_g values growing until an approximate plateau is reached. Note that the slight reduction occurring during the plateau period is due to the thermal degradation or oxidative crosslinking behaviour caused by high curing temperatures. This was also observed experimentally by Carbas et al. [31]. The variation in the modulus values (Figure 8 (b)) is relatively small (noting the different vertical scale ratios), with a

289 general tendency to increase with increasing curing temperature. The fluctuations in
290 the modulus values are partly caused by the combined errors in the collected
291 different experimental data and the training process (see Figure 6 (b) and (d)).

- 292 • Similarly, as the curing time increases from 3 days, the predicted T_g values continue
293 to increase until they approach an approximate plateau, as shown in Figure 8 (c).
294 The modulus values (mainly E1, E2, and E3), however, decrease firstly and then
295 increase (see Figure 8 (d)).
- 296 • The humidity is detrimental to the thermal performance of the adhesive, as indicated
297 in Figure 8 (e) and (f). Both the T_g and the modulus reduce as the curing humidity
298 increases from 0% RH to 100% RH.

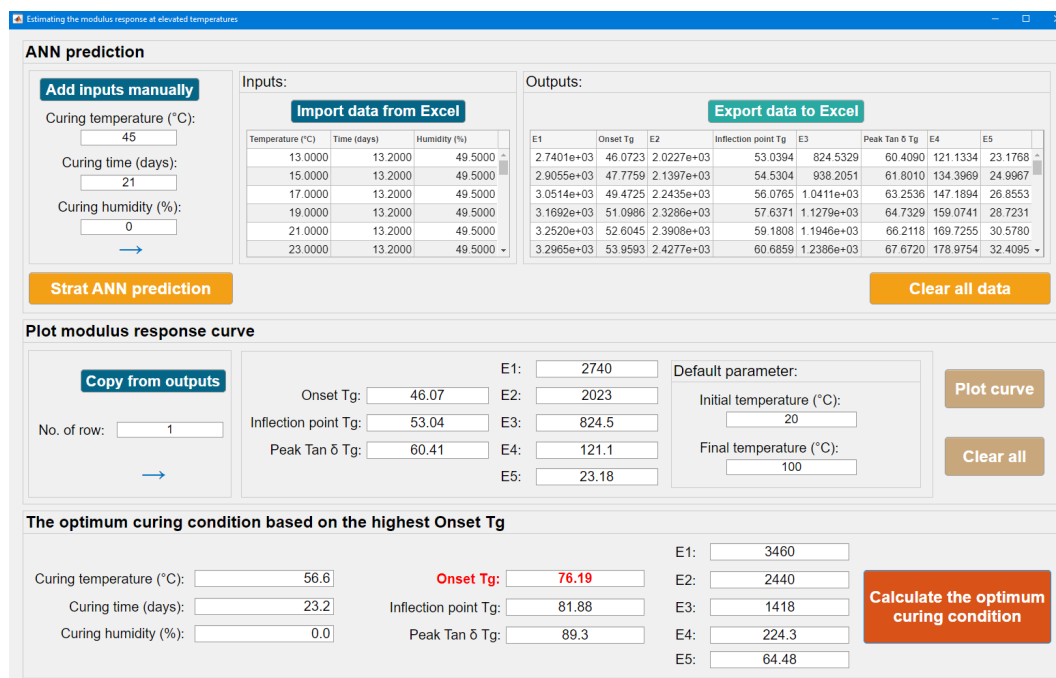
299 The curing conditions have a significantly impact on the temperature at which the glass
300 transition behaviour of the adhesive begins, however, the impact on the specific modulus values
301 at different stages of its transition from the glassy state to the rubbery state is limited. Curing
302 the adhesive at an extremely high temperature over a long period of time is not conducive to
303 practical engineering applications and this does not necessarily lead to a better thermal
304 performance due to the thermal degradation or oxidative crosslinking effect. As a result, cured
305 at an adequate warm temperature (≥ 45 °C) for around 21 days is sufficient for the studied
306 adhesive, and the curing is preferably conducted in a dry environment.

307

308 **6 Graphical User Interface (GUI) design**

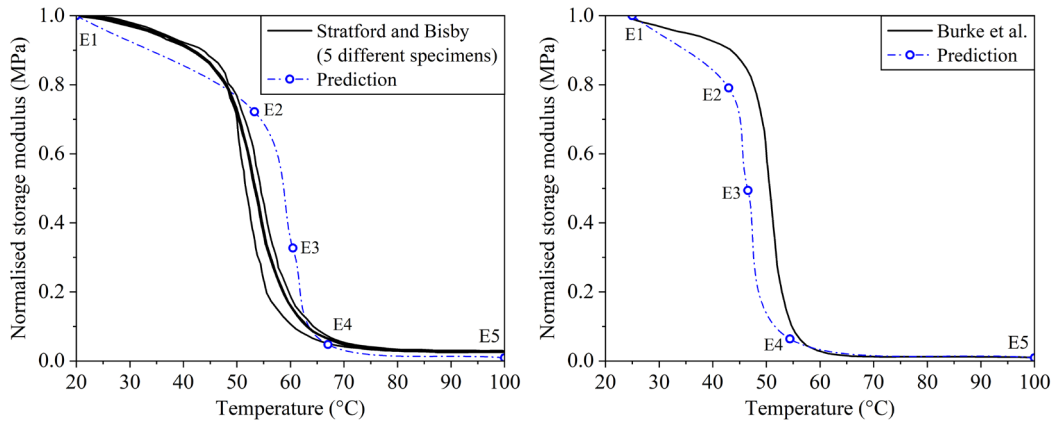
309 Applying the original ANN model requires further coding work, which could be an obstacle
310 for civil engineers. Establishing a user-friendly software that implements the developed ANN
311 model can facilitate turning machine learning results into practical applications. The designed
312 software with a GUI was programmed using MATLAB, and the source code is publicly
313 available in the supplementary material.

314 As shown in Figure 9, the software is capable of predicting the different modulus responses
 315 of the adhesive according to the different applied curing conditions. The modulus response
 316 curve can be generated based on the selected set of output values. In addition, the optimum
 317 curing condition can be calculated with respect to the maximum onset, T_g , at which the modulus
 318 of the adhesive starts to drop significantly. The optimum curing condition is estimated to be
 319 cured at 56.6 °C and 0% RH for 23.2 days, which agrees with the recommendation proposed
 320 at the end of Section 5. Utilising these functions of the software can provide more
 321 comprehensive results on the response of the adhesive.



322
323 Figure 9: GUI for estimation of the modulus response at elevated temperatures

324 The effectiveness of the software was validated by comparing the predicted results with the
 325 experimental results from two references separately, as shown in Figure 10. The results in these
 326 2 references were not used in training the ANN model (unlike in Figure 7), which ensures a
 327 reasonable validation.



(a) compared with the experimental results in [7] (b) compared with the experimental results in [44]
 Figure 10: Validation of the established software

328
 329
 330

331 Whilst the errors in the specific T_g values are approximately $\pm 5^\circ\text{C}$, the shape of the curve
 332 representing the tendency of the modulus to decrease at elevated temperatures can be well
 333 estimated. The software can be upgraded when more data is available to train a more robust
 334 ANN model and to include consideration of different chemical formulations for different types
 335 of structural adhesives. The current version can be used as a simple tool to conveniently
 336 estimate the approximate modulus response of the adhesive based on the applied curing
 337 condition, without the need for experimentation; however, caution is necessary in applying this
 338 software to obtain specific T_g or modulus values.

339

340 7 Conclusions

341 This study proposes using the machine learning approach for analysing and predicting the
 342 storage modulus response of the structural epoxy adhesive (Sikadur-330 [32]) at elevated
 343 temperatures. By utilising its powerful data processing and inductive learning capabilities, the
 344 links between parameters and results are inferred and analysed, which enables us to gain a
 345 deeper understanding of the patterns implied in the extensive experimental results.

346 An artificial neural network model was developed to map the relationship between the
 347 modulus response and the applied curing conditions, and to provide predicted reference values
 348 for practical engineering applications. The analytical results of the ANN model were verified

349 against the published experimental studies, demonstrating the powerful generalisation and
350 prediction capabilities of the ML model. The sensitivity analysis of variables was performed
351 based on the massive prediction results generated using the ANN model.

- 352 • The effects of curing conditions on the T_g results of the adhesive are more significant
353 than those on the modulus results. As the curing temperature or curing time increases,
354 the T_g values will increase until the thermal energy is sufficient to complete the
355 crosslinking, leading to an approximate plateau.
- 356 • Increasing curing humidity can result in a decrease in the T_g and modulus, which is
357 detrimental to the thermal performance of the adhesive.
- 358 • It is recommended to cure the studied adhesive at a warm temperature (≥ 45 °C) and
359 in a dry environment (close to 0% RH) for around 21 days in practical applications.

360 A user-friendly software with a Graphical User Interface (GUI) has been established by
361 implementing the ANN model. The efficiency and capability of this simple tool have been
362 illustrated. Using its powerful computational capabilities, the optimum curing condition for the
363 examined adhesive was estimated to be 23.2 days at 56.6 °C and 0% RH. However,
364 experimental confirmation would be required when using the software for design purposes.

365 Like any other machine learning method, the generalisability of the ANN model might be
366 limited to the range of the dataset used. The dataset is expected to be updated as more
367 experimental data becomes available to train a more robust ANN model and to consider
368 different chemical formulations for different types of structural adhesives. Nevertheless, the
369 present study demonstrates the use of a machine learning approach to comprehensively analyse
370 and predict the modulus response of a structural epoxy adhesive according to the applied curing
371 condition.

372

373 **Acknowledgments**

374 The authors are grateful for the support from the International Collaborative Research Fund
375 for Young Scholars in the Innovation Demonstration Base of Ecological Environment
376 Geotechnical and Ecological Restoration of Rivers and Lakes. This work was funded by the
377 Doctoral Research Starting Foundation of Hubei University of Technology under Grant
378 [XJ2022001301].

379

380 **Disclosure statement**

381 The authors report there are no competing interests to declare.

382

383 **Funding**

384 This work was supported by the Doctoral Research Starting Foundation of Hubei University
385 of Technology under Grant [XJ2022001301].

386

387 **Data availability statement**

388 The supplementary material that supports the findings of this study is publicly available in
389 *figshare* at <https://doi.org/10.6084/m9.figshare.21640772.v1>.

390

391 **References**

392 [1] Teng, J. G.; Yu, T.; Fernando, D. Strengthening of steel structures with fiber-reinforced polymer composites. *J Constr*
393 *Steel Res.* 2012, 78:131–43. <https://doi.org/10.1016/j.jcsr.2012.06.011>.

394 [2] Al-Saadi, N. T. K.; Mohammed, A.; Al-Mahaidi, R.; Sanjayan, J. A state-of-the-art review: Near-surface mounted
395 FRP composites for reinforced concrete structures. *Constr Build Mater.* 2019, 209:748–69.
396 <https://doi.org/10.1016/j.conbuildmat.2019.03.121>.

397 [3] Wang, S.; Stratford, T.; Reynolds, T. P. S. A comparison of the influence of nonlinear and linear creep on the
398 behaviour of FRP-bonded metallic beams at warm temperatures. *Compos Struct.* 2022, 281:115117.
399 <https://doi.org/10.1016/j.compstruct.2021.115117>.

400 [4] Banea, M. D.; Da-Silva, L. F. M. Mechanical characterization of flexible adhesives. *J Adhes.* 2009, 85:261–85.
401 <https://doi.org/10.1080/00218460902881808>.

- 402 [5] Gu, Z.; Liu, Y.; Hughes, D. J.; Ye, J.; Hou, X. A parametric study of adhesive bonded joints with composite material
403 using black-box and grey-box machine learning methods: Deep neuron networks and genetic programming. *Compos*
404 *Part B Eng.* 2021, 217:108894. <https://doi.org/10.1016/j.compositesb.2021.108894>.
- 405 [6] He, J.; Xian, G.; Zhang, Y. X. Numerical modelling of bond behaviour between steel and CFRP laminates with a
406 ductile adhesive. *Int J Adhes Adhes.* 2021, 104:102753. <https://doi.org/10.1016/j.ijadhadh.2020.102753>.
- 407 [7] Stratford, T. J.; Bisby, L. A. Effect of warm temperatures on externally bonded FRP strengthening. *J Compos Constr.*
408 2012, 16:235–44. [https://doi.org/10.1061/\(ASCE\)CC.1943-5614.0000260](https://doi.org/10.1061/(ASCE)CC.1943-5614.0000260).
- 409 [8] Marques, E. A. S.; Da-Silva, L. F. M.; Banea, M. D.; Carbas, R. J. C. Adhesive joints for low- and high-temperature
410 use: An overview. *J Adhes.* 2014, 91:556–85. <https://doi.org/10.1080/00218464.2014.943395>.
- 411 [9] Hisham, M.; Hamdy, G. A.; El-Mahdy, O. O. Prediction of temperature variation in FRP-wrapped RC columns
412 exposed to fire using artificial neural networks. *Eng Struct.* 2021, 238:112219.
413 <https://doi.org/10.1016/j.engstruct.2021.112219>.
- 414 [10] Wang, S.; Stratford, T.; Reynolds, T. P. S. Linear creep of bonded FRP-strengthened metallic structures at warm
415 service temperatures. *Constr Build Mater.* 2021, 283:122699. <https://doi.org/10.1016/j.conbuildmat.2021.122699>.
- 416 [11] Cree, D.; Gamaniouk, T.; Loong, M. L.; Green, M. F. Tensile and Lap-Splice Shear Strength Properties of CFRP
417 Composites at High Temperatures. *J Compos Constr.* 2015, 19:04014043. [https://doi.org/10.1061/\(asce\)cc.1943-5614.0000508](https://doi.org/10.1061/(asce)cc.1943-5614.0000508).
- 419 [12] Huang, J. S.; Liew, J. X.; Liew, K. M. Data-driven machine learning approach for exploring and assessing mechanical
420 properties of carbon nanotube-reinforced cement composites. *Compos Struct.* 2021, 267:113917.
421 <https://doi.org/10.1016/j.compstruct.2021.113917>.
- 422 [13] Su, M.; Zhong, Q.; Peng, H.; Li, S. Selected machine learning approaches for predicting the interfacial bond strength
423 between FRPs and concrete. *Constr Build Mater.* 2021, 270:121456.
424 <https://doi.org/10.1016/j.conbuildmat.2020.121456>.
- 425 [14] Samuel, A. L. Machine learning. *Technol Rev.* 1959, 62:42–5.
- 426 [15] Sharma, A.; Mukhopadhyay, T.; Rangappa, S. M.; Siengchin, S.; Kushvaha, V. Advances in Computational
427 Intelligence of Polymer Composite Materials: Machine Learning Assisted Modeling, *Analysis and Design*. Vol, 29,
428 2022. <https://doi.org/10.1007/s11831-021-09700-9>.
- 429 [16] Ghaboussi, J.; Garrett, J. H.; Wu, X. . Knowledge-based modeling of material behavior with neural networks. *J Eng*
430 *Mech.* 1991, 117(1):132–53. [https://doi.org/10.1061/\(ASCE\)0733-9399\(1991\)117:1\(132\)](https://doi.org/10.1061/(ASCE)0733-9399(1991)117:1(132)).
- 431 [17] Rao, H. S.; Mukherjee, A. Artificial neural networks for predicting the macromechanical behaviour of ceramic-matrix
432 composites. *Comput Mater Sci* 1996, 5:307–22. [https://doi.org/10.1016/0927-0256\(95\)00002-X](https://doi.org/10.1016/0927-0256(95)00002-X).
- 433 [18] Sommer, D.; Haufe, A.; Middendorf, P. A machine learning material model for structural adhesives in finite element
434 analysis. *Int J Adhes Adhes.* 2022, 117. <https://doi.org/10.1016/j.ijadhadh.2022.103160>.
- 435 [19] Mashrei, M. A.; Seracino, R.; Rahman, M. S. Application of artificial neural networks to predict the bond strength of
436 FRP-to-concrete joints. *Constr Build Mater.* 2013, 40:812–21. <https://doi.org/10.1016/j.conbuildmat.2012.11.109>.
- 437 [20] Tosun, E.; Çalik, A. Failure load prediction of single lap adhesive joints using artificial neural networks. *Alexandria*

- 438 *Eng J.* 2016, 55:1341–6. <https://doi.org/10.1016/j.cej.2016.04.029>.
- 439 [21] Zgoul, M. H. Use of artificial neural networks for modelling rate dependent behaviour of adhesive materials. *Int J*
440 *Adhes Adhes.* 2012, 36:1–7. <https://doi.org/10.1016/j.ijadhadh.2012.03.003>.
- 441 [22] Jha, A.; Chandrasekaran, A.; Kim, C.; Ramprasad, R. Impact of dataset uncertainties on machine learning model
442 predictions: The example of polymer glass transition temperatures. *Model Simul Mater Sci Eng.* 2019, 27.
443 <https://doi.org/10.1088/1361-651X/aaf8ca>.
- 444 [23] Tao, L.; Chen, G.; Li, Y. Machine learning discovery of high-temperature polymers. *Patterns.* 2021, 2:100225.
445 <https://doi.org/10.1016/j.patter.2021.100225>.
- 446 [24] Szabelski, J.; Karpiński, R.; Machrowska, A. Application of an Artificial Neural Network in the Modelling of Heat
447 Curing Effects on the Strength of Adhesive Joints at Elevated Temperature with Imprecise Adhesive Mix Ratios.
448 *Materials (Basel).* 2022, 15. <https://doi.org/10.3390/ma15030721>.
- 449 [25] Paiva, R. M. M.; António, C. A. C.; Da-Silva, L. F. M. Sensitivity and optimization of peel strength based on
450 composition of adhesives for footwear industry. *J Adhes.* 2015, 91:801–22.
451 <https://doi.org/10.1080/00218464.2014.971119>.
- 452 [26] Géron, A. *Hands-On Machine Learning with Scikit-Learn, Keras, and TensorFlow: Concepts, Tools, and Techniques*
453 *to Build Intelligent Systems*; O'Reilly Media, 2022.
- 454 [27] Shalev-Shwartz, S.; Ben-David, S. *Understanding machine learning: From theory to algorithms*; Cambridge
455 University Press, 2014.
- 456 [28] Moradi, M. J.; Daneshvar, K.; Ghazi-nader, D.; Hajiloo, H. The prediction of fire performance of concrete-filled steel
457 tubes (CFST) using artificial neural network. *Thin-Walled Struct.* 2021, 161.
458 <https://doi.org/10.1016/j.tws.2021.107499>.
- 459 [29] Lecun, Y.; Bengio, Y.; Hinton, G. Deep learning. *Nature.* 2015, 521:436–44. <https://doi.org/10.1038/nature14539>.
- 460 [30] Menard, K. P. *Dynamic mechanical analysis: a practical introduction*; Boca Raton: Taylor & Francis Group, 2020.
- 461 [31] Carbas, R. J. C.; Marques, E. A. S.; Da-Silva, L. F. M.; Lopes, A. M. Effect of cure temperature on the glass transition
462 temperature and mechanical properties of epoxy adhesives. *J Adhes.* 2014, 90:104–19.
463 <https://doi.org/10.1080/00218464.2013.779559>.
- 464 [32] SIKA. *Sikadur®-330 Data Sheet*; Sika Construction Chemicals, 2017.
- 465 [33] Sousa, J. M.; Correia, J. R.; Gonilha, J.; Cabral-Fonseca, S.; Firmo, J. P.; Keller, T. Durability of adhesively bonded
466 joints between pultruded GFRP adherends under hygrothermal and natural ageing. *Compos Part B Eng.* 2019,
467 158:475–88. <https://doi.org/10.1016/j.compositesb.2018.09.060>.
- 468 [34] Liu, X.; Tian, S.; Tao, F.; Yu, W. A review of artificial neural networks in the constitutive modeling of composite
469 materials. *Compos Part B Eng.* 2021, 224:109152. <https://doi.org/10.1016/j.compositesb.2021.109152>.
- 470 [35] Wang, S.; Stratford, T.; Reynolds, T. P. S. FRP-strengthened metallic beams under temperature cycles. In Proceedings
471 of the 15th International Conference on Fibre-Reinforced Polymers for Reinforced Concrete Structures (FRPRCS-
472 15) & The 8th Asia-Pacific Conference on FRP in Structures (APFIS-2022), Shenzhen, China, 10-14 December 2022.

- 473 [36] Adams, R. D. (Ed), *Adhesive bonding: science, technology and applications*; Woodhead Publishing Limited:
474 Cambridge, England, 2021.
- 475 [37] *Origin Pro*, version 2016 Academic; Origin Lab Corporation: Northampton, USA, 2016.
- 476 [38] Othman, D. J. Influence of adhesive curing temperature upon the performance of FRP strengthened steel structures
477 at ambient and elevated temperatures. Ph.D. Dissertation, The University of Edinburgh, Edinburgh, U.K., 2017.
- 478 [39] Seif, C. Y.; Hage, I. S.; Hamade, R. F. Weibull reliability plots to study the strain rate effect on interfacial strengths
479 of carbon fiber reinforced epoxy composites. *Polym Compos.* 2022, 2022:1–13. <https://doi.org/10.1002/pc.26888>.
- 480 [40] Sun, W.; Vassilopoulos, A. P.; Keller, T. Effect of thermal lag on glass transition temperature of polymers measured
481 by DMA. *Int J Adhes Adhes.* 2014, 52:31–9. <https://doi.org/10.1016/j.ijadhadh.2014.03.009>.
- 482 [41] Verdet, M.; Salenikovich, A.; Cointe, A.; Coureau, J. L.; Galimard, P.; Toro, W. M. Mechanical Performance of
483 Polyurethane and Epoxy Adhesives in Connections with Glued-in Rods at Elevated Temperatures. *BioResources.*
484 2016, 11:8200–14. <https://doi.org/10.15376/BIORES.11.4.8200-8214>.
- 485 [42] Lartigau, J.; Coureau, J. L.; Morel, S.; Galimard, P.; Maurin, E. Effect of temperature on the load bearing capacity of
486 glued-in rods. In Proceedings of the World Conference on Timber Engineering 2012 (WCTE 2012), Auckland, New
487 Zealand, 16–19 July 2012.
- 488 [43] Savvilotidou, M. Durability and fatigue performance of a typical cold-curing structural adhesive in bridge
489 construction. Ph.D. Dissertation, Swiss Federal Institute of Technology Lausanne, Vaud, Switzerland, 2017.
- 490 [44] Burke, P. J.; Bisby, L. A.; Green, M. F. Effects of elevated temperature on near surface mounted and externally
491 bonded FRP strengthening systems for concrete. *Cem Concr Compos.* 2013, 35:190–9.
492 <https://doi.org/10.1016/j.cemconcomp.2012.10.003>.
- 493 [45] Hu, L.; Feng, P.; Meng, Y.; Yang, J. Buckling behavior analysis of prestressed CFRP-reinforced steel columns via
494 FEM and ANN. *Eng Struct.* 2021, 245:112853. <https://doi.org/10.1016/j.engstruct.2021.112853>.
- 495 [46] Gouravaraju, S.; Narayan, J.; Sauer, R. A.; Gautam, S. S. A Bayesian regularization-backpropagation neural network
496 model for peeling computations. *J Adhes.* 2021, 00:1–24. <https://doi.org/10.1080/00218464.2021.2001335>.
- 497